2023 IEEE International Conference on Environment and Electrical Engineering and 2023 IEEE Industrial and Commercial Power Systems Europe (EEEIC / I&CPS Europe) | 979-8-3503-4743-2/23/$31.00 ©2023 IEEE | DOI: 10.1109/EEEIC/ICPSEUROPE57605.2023.10194881

Automatic Generation Control via Hydrogen Storage Power Plants in a Nodal Voltage Angle Controlled Grid

Nayeemuddin Ahmed, Harald Weber
Institute for Electrical Power Engineering
University of Rostock
Rostock, Germany
{nayeemuddin.ahmed, harald.weber}@uni-rostock.de

***Abstract*—Electrical Energy Storage (EES) systems have progressively gained prominence as a means to large-scale integration of intermittent Renewable Energy Sources (RES). The Hydrogen Storage Power Plant (HSPP) is one solution that can autonomously supply or store electrical energy in bulk according to the requirements of the network. Previous investigations have verified the ability of this power plant to provide the required ancillary services in the form of instantaneous and primary control reserves to ensure a stable system regulated via voltage angle control. However, since this novel regulation method always maintains the grid frequency near the rated value, controlling interchange power in grids with multiple control areas was an unsolved problem. In conventional frequency-controlled systems, this goal is achieved using an Automatic Generation Controller, which operates on frequency deviation. However, the lack of such a frequency difference in an angle-controlled grid means an alternative control model would be required. Thus, in this paper, a new AGC model has been recommended, which, when connected to a HSPP, enables the power plant to continuously regulate the interchange power under voltage angle control.**

***Index Terms*—Ancillary service, automatic generation control, hydrogen storage, frequency control, voltage angle control**

I. Introduction

According to the current German Renewable Energy Sources (RES) Act, renewable resources are expected to support 80% of the country's gross electricity consumption by 2030 [1]. Though deemed necessary for climate protection, such high penetration of RES (primarily wind and solar for Germany) introduces additional challenges in regulating the electrical power system. A major drawback of RES is its dependency on the fluctuating primary resource to generate electrical power. As a result, such resources cannot always meet the grid demand [2]. Currently, the difference between intermittent electrical power generation from RES and consumption by loads is bridged by conventional power plants (CPP). However, most of these plants being coal-fired are planned to be phased out and completely replaced with RES by 2038 in Germany. Thus, to ensure grid stability, alternate solutions are needed in the futuristic power system to provide the required ancillary services, as currently done by CPPs.

979-8-3503-4743-2/23/$31.00 ©2023 IEEE

One such solution is the Hydrogen Storage Power Plant (HSPP). This consists of an interconnected system of converters and storages. The arrangement of these components ensures that the power plant can supply electrical energy per the grid requirement and store it during periods of excess RES infeed. Such properties enable the HSPP to neutralize the intermittency of RES. There are three main storages inside the plant, i.e., supercapacitor, battery and hydrogen storage. Each of these is ideally suited for providing instantaneous, primary and secondary control reserve (IR, PCR, SCR). This enables the HSPP to provide the necessary ancillary actions [3].

The current electrical grid possesses many inverter-interfaced RES and CPP with large rotating masses. Due to these large masses, there is an inherent link between the active power balance and grid frequency. However, after nuclear and coal-fired CPP shutdown, power generation will primarily depend on RES, Storage and High Voltage Direct Current (HVDC) systems. The decoupling of such generation sources from the system frequency due to their power electronic interface means that in such a situation, the electrical network can be operated at a constant frequency, e.g., 50 Hz. IR, PCR, and SCR, which are currently dependent on frequency changes, would instead be fulfilled using the voltage angle at the power plant's interfacing converter. This novel grid control strategy is called the "Nodal Voltage Angle Control" [4].

The IR and PCR provision under this new regulation technique has been discussed in [4]. However, satisfying all the SCR goals has remained a challenge. Due to the absence of a definitive frequency deviation in this method, conventional Automatic Generation Control (AGC) schemes cannot be used to control the interchange power between different control areas. Thus, in this paper, a modified AGC mechanism has been proposed and implemented in HSPPs, which continuously regulates the exchange power between multiple areas. The following sections explain and prove the functionality of this proposed model in a standard IEEE network.

II. Test Electrical Network

A standard network with multiple control areas is required to test the new AGC structure. Thus, the 400 kV transmission system available as an example in the simulation software DIgSILENT PowerFactory is used. A simplified representation is presented in Fig. 1. The chosen network has 4 control areas named North West (NW), North East (NE), South West (SW) and South East (SE). Each represents the power grid around a major city in southern Germany [5]. Every control area is represented by three sites, numbered 01 to 03. A single circle represents sites containing only loads, while those containing only generation or both generation and loads are represented with concentric circles.

In the example [5], the power generation in the different sites of each control area mostly relies on synchronous generators. To depict a futuristic scenario, all but two synchronous generators in the interconnected network are replaced by converter systems representing wind farms and HSPPs. These synchronous generators (one in SW and another in SE) remain in the grid, supplying part of the base load so that their response under voltage angle control can be investigated. The initial load flow results for each control area are summarized in Table I. The resulting power flow over the tie lines interconnecting different control areas due to these operating points is also shown in Fig. 1.

In this analysis, the loads and wind farms are represented as PQ nodes, i.e., points where the active (P) reactive (Q) powers are controlled. The synchronous generators are denoted as PV nodes, i.e., terminals where the active power (P) and voltage magnitude ($|V|$) are controlled. The HSPPs (located at sites marked in green) are represented as slack nodes, where the voltage magnitude ($|V|$) and angle (ϕ_U) are kept constant.

Dynamic controllers (P-ϕ_U, Q-V and AGC) are designed to ensure that only the HSPPs in the respective control areas meet the required IR, PCR and SCR provisions. Thus, whenever there are disturbances in the system, the HSPPs adapt their power output to satisfy the changes in demand and regulate

TABLE I
INITIAL POWER FLOW SUMMARY OF DIFFERENT CONTROL AREAS

Control area	Active power generation (MW)	Active power consumption (MW)	Losses (MW)	No. of HSPP
NW	82.3	1600	1.35	1
NE	1895.9	1900	13.88	2
SW	2599.5	1196.8	19.04	2
SE	1509.7	1350	6.33	2
Total	**6087.4**	**6046.8**	**40.6**	**7**

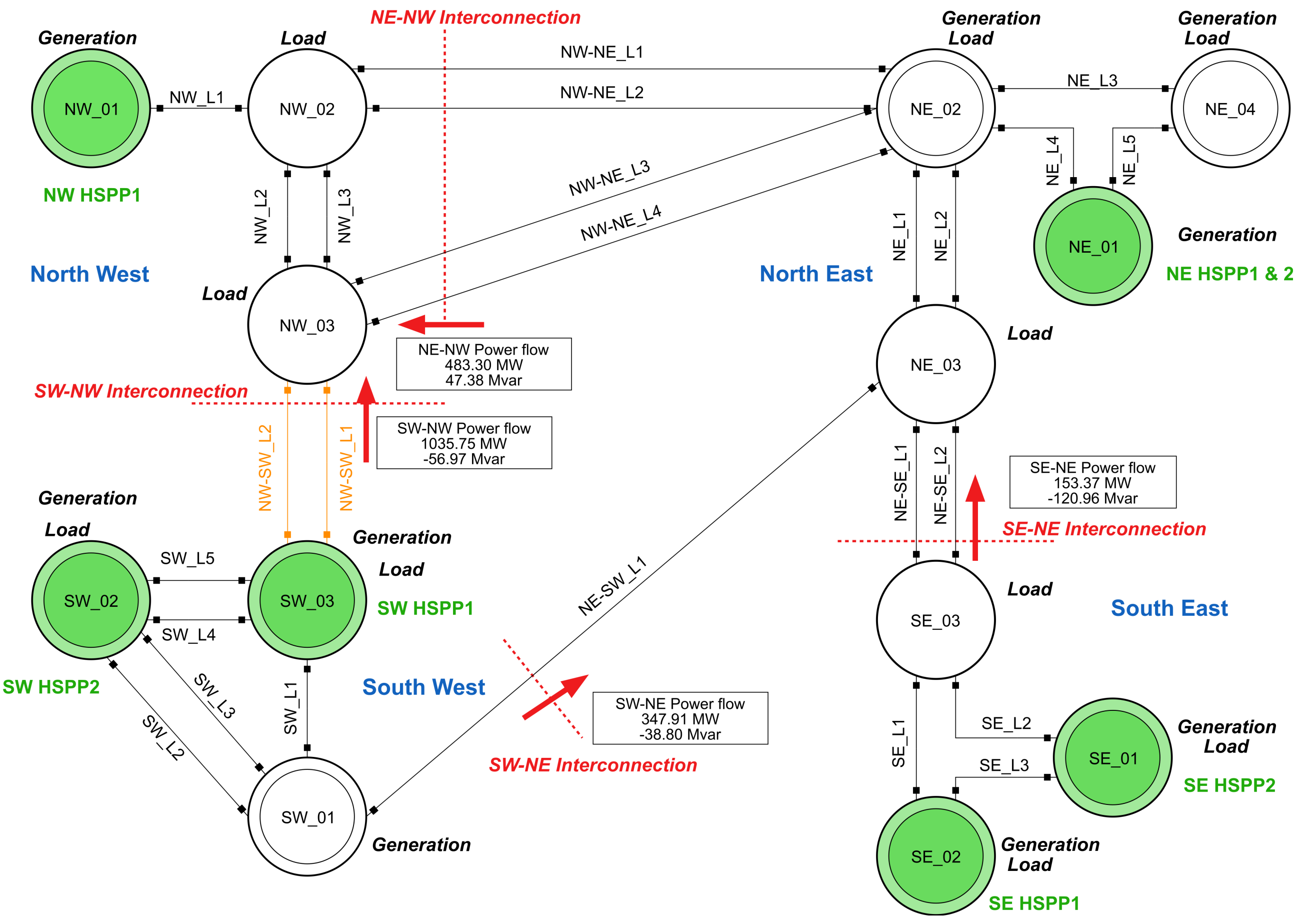

Fig. 1. 400 kV transmission system in DIgSILENT PowerFactory [5]

the power exchange between the different control areas with minimal frequency deviation. This enables the wind farms to continuously operate at their maximum power point (maximizing revenue), i.e., without maintaining a constant reserve for ancillary services. Furthermore, the synchronous generators can operate at base load, ensuring economical dispatch.

III. Internal HSPP Structure

The internal HSPP structure is presented in Fig. 2. In such power plants, following an active power imbalance in the three-phase network, the tasks of providing IR, PCR and SCR are accomplished by the three main storages, i.e., supercapacitor, battery and hydrogen storage, respectively [3], [6], [7]. A supercapacitor provides IR since the component can charge and discharge instantaneously with a high power gradient in response to network disturbances. In addition, its ability to undergo frequent charging and discharging cycles makes it an ideal device for inertia emulation [8].

The voltage of the supercapacitor is controlled to govern the PCR from the battery using the adjacent DC-DC converter. Contrary to the supercapacitor, the battery is suited for PCR provision since it is a cheaper form of storage with a higher energy density. Rapid charging or discharging of the battery is detrimental to its average lifespan, so the use of battery systems for providing IR is still unproven [9]. Hence, the combination of the supercapacitor in parallel to the battery satisfies the required IR and PCR requirements.

The battery voltage is regulated to direct the SCR response from the hydrogen storage. If there is surplus energy in the network, e.g., due to increased RES infeed, the battery voltage rises. After exceeding an upper threshold, the electrolyser path (in Fig. 2) is activated. The excess energy is then used to synthesize hydrogen and transfer it to the storage. In case of increased demand, if the battery voltage reduces beyond a lower threshold after providing PCR, the fuel cell path is activated. SCR provisions are then met by the fuel cell generating electrical energy from the stored hydrogen. The power flow, during each situation, is controlled by the respective DC-DC converter between the hydrogen storage and the battery. In this way, the HSPP adapts its active power output during positive and negative disturbances ensuring stability.

The hydrogen produced via electrolysis can be stored in a Liquid Organic Hydrogen Carrier (LOHC) system. Such a system enables safe storage and transportation of hydrogen at a high energy density under ambient conditions using the currently available infrastructure [10]. In addition to being used in the HSPP, the stored hydrogen can play a vital role in sector coupling (Power-to-X) and industrial decarbonization.

IV. AGC Model

The primary functions of conventional AGCs include [11]:

1) Restoration of the system frequency to its nominal value following a large disturbance
2) Regulation of the interchange power between control areas to scheduled values by adjusting the output of the related power plants

In a conventional system, the interchange power is restored to specified setpoints (per agreed contracts) using the frequency deviation. However, in an angle-controlled grid, the frequency always stays near the nominal value (50 Hz in the ENTSO-E region). Hence, the main goal of this novel AGC is to regulate the interchange power between the control areas independent of the frequency deviation. This is achieved by extracting the required signal from the modified AGC and transmitting it to the HSPP.

Under normal circumstances, the HSPP operates in slack mode, regulating its voltage magnitude and angle (ϕ_U) to a constant value. This enables it to provide only IR and PCR. Once the AGC output is sent to the HSPP, it changes its mode of operation from slack to PQ, controlling active (P) and reactive (Q) power, as shown in Fig. 3. The HSPP then changes its voltage angle and, along with IR and PCR, also provides SCR to regulate the interchange power. The following section illustrates the function of this novel control model.

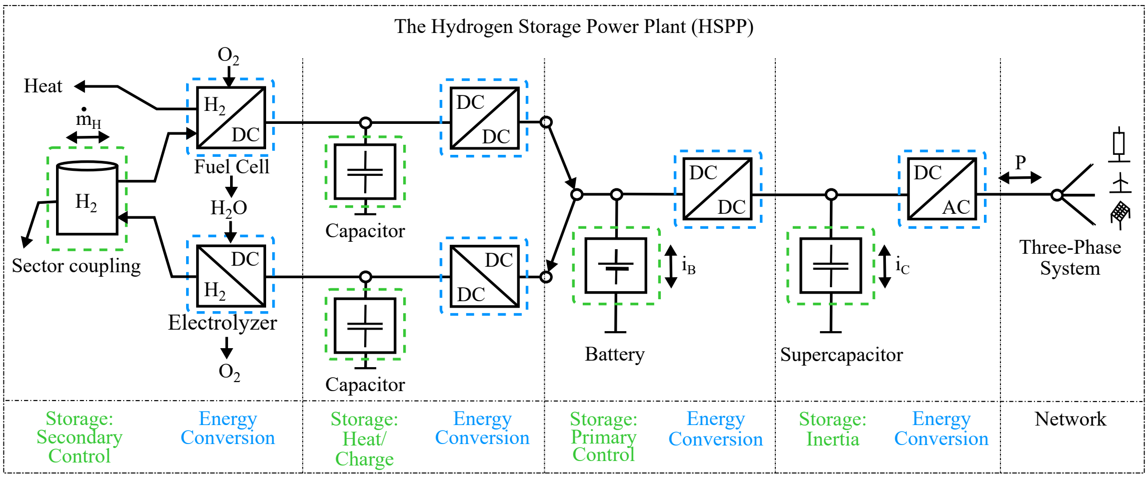

Fig. 2. Working principle of the internal components of a Hydrogen Storage Power Plant (HSPP)

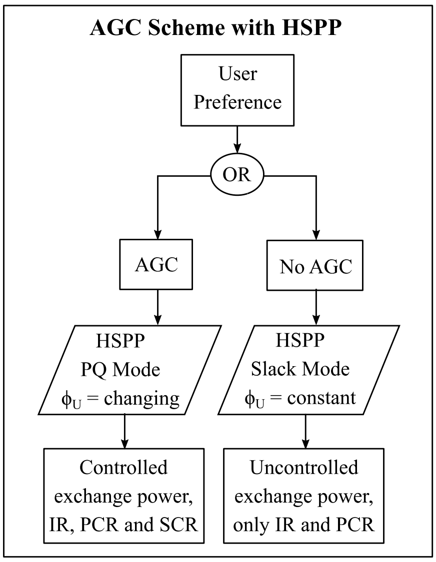

Fig. 3. Process flow of the AGC

V. RESULT AND OBSERVATION

To test the novel AGC scheme, a load profile characteristic is implemented in load 03 of the Northwestern control area. This represents power consumption on a typical summer weekday in Germany. The change in active power consumption is shown in Fig. 4a. The power demand of the other loads in the system is kept constant. Due to the initial increase in power consumption at the load node, the angular speed of the voltage phasor and hence the frequency at the load busbar decreases. This is shown in Fig. 4b. Alternatively, when the load power consumption decreases (to negative values), the frequency at the connecting busbar increases.

At first, the responses of the HSPPs are analyzed, excluding an AGC so its effect can be compared later. Thus, without an AGC, all the HSPPs function as pure slack nodes and keep their voltage angles constant at the reference value received from the initial load flow, as discussed in Table I. As a result, the frequency always remains at the nominal value of 50 Hz at every HSPP point of connection. Since plotting multiple HSPP frequency curves on the same diagram would result in overlap, the frequency of only one HSPP in NW is presented in Fig. 4b.

Figs. 4c & d depict the power change of the HSPPs due to the change in load power consumption. Since the HSPPs maintain their initial voltage angles throughout the simulation, the additional power provided or consumed to meet the changing load demand is load flow oriented. This means the HSPPs close to load 03 in NW provide a greater response than the ones further away. Thus according to the results, the HSPPs in NW and SW are closer to load 03 than the ones in NE and SE. The grid representation in Fig. 1 supports these findings. Hence, under voltage angle control, IR and PCR provisions are primarily met by HSPPs closer to the location of the disturbance. The local provision of such

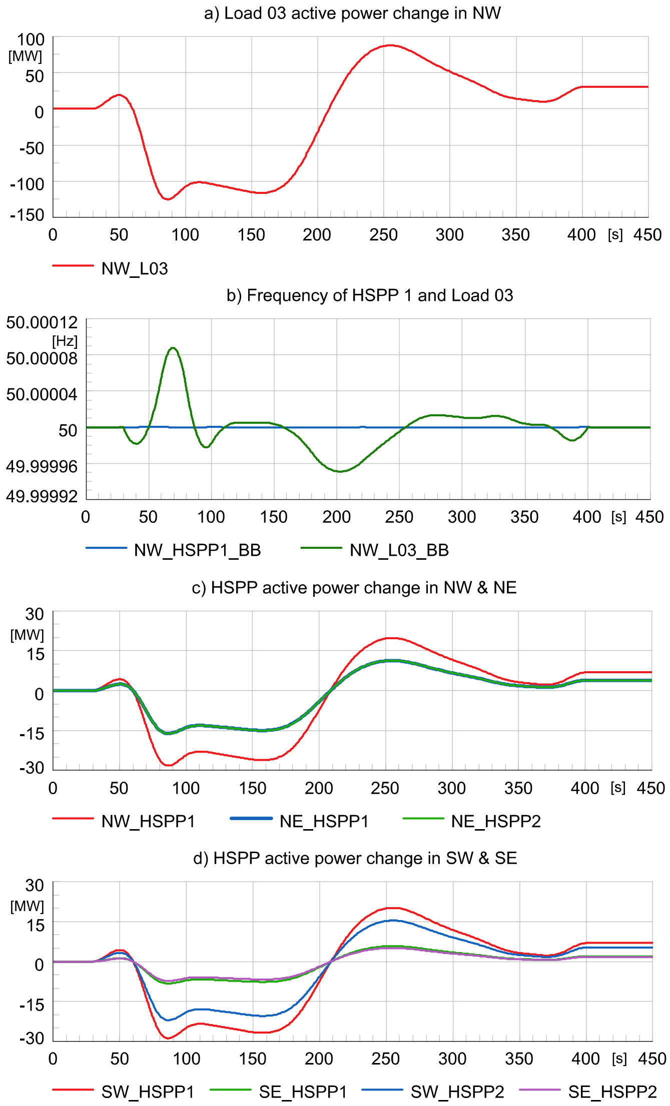

Fig. 4. a) Active power of load 03 in North West control area, b) Frequency changes at load 03 and HSPP 1 busbar in the same control area, c) & d) Resulting generator responses in different control areas **without AGC**

ancillary actions restricts the power flow close to the source of the change. This prevents the overloading of distant HSPPs and transmission lines.

The HSPP active power responses can be further explained by Fig. 5, which shows the voltage angle deviations for all sites. The nodes connected to HSPPs (highlighted in green) do not show any change in the voltage angle since HSPPs act as slacks. The largest change is observed at NW_03, which houses load 03. An increase in the power consumption by load 03 leads to a reduction in its voltage angle. Since the nearby slacks keep their voltage angles constant, this leads to an increase in the voltage angle difference between two neighboring nodes, resulting in a higher power flow to the load. Similarly, a decrease in the load power consumption leads to an increase in its voltage angle and a consequent power flow to the nearby slack nodes (NW_HSPP1, SW_HSPP1 & 2).

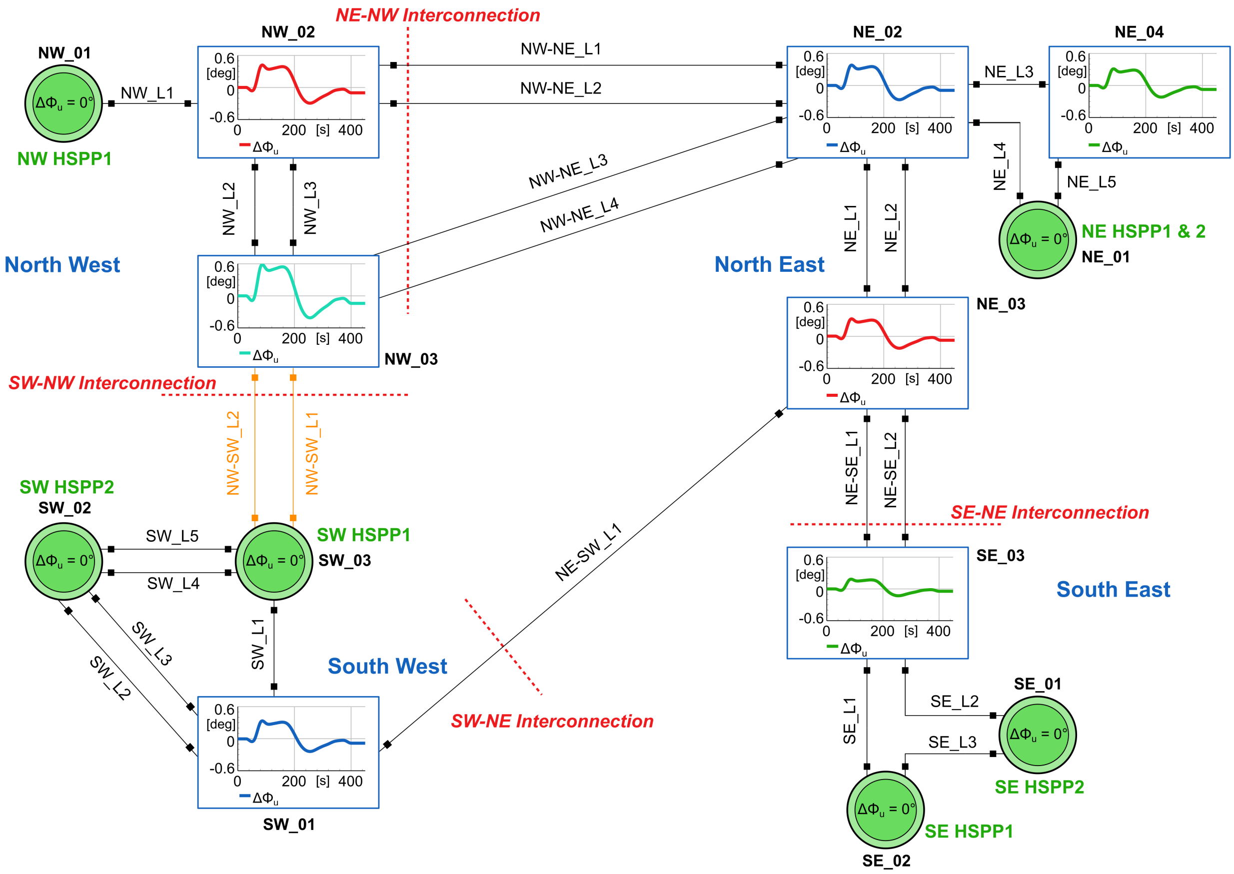

Fig. 5. 400 kV transmission system grid in DIgSILENT PowerFactory with voltage angles deviations for non-slack nodes [5]

Generally, the voltage angles at the non-slack sites follow the trend in NW_03 to maintain a constant power flow between the sites. Distant points such as SE_03 exhibit significantly lower voltage angle changes compared to NW_03 due to the large impedance between the two sites. As a result, the slacks in SE react to a smaller voltage angle change and provide a lower change in their active power outputs, as seen in Fig. 4d.

Next, the system response to the same load change is analyzed in the presence of an AGC. As shown in Fig. 4a, a slow disturbance pattern is intentionally chosen to evaluate the AGC performance since it minimizes the IR and PCR requirements and highlights the HSPP's SCR response. As shown in Fig. 6a, the frequency change at load 03 busbar has the same trend as before. However, in this case, the modified AGC recognizes that the disturbance is in NW after measuring the interchange power deviation in every control area. To provide SCR, a signal is then sent to the HSPPs to switch from slack to PQ mode. In addition, a new power reference is created for each HSPP, which leads large change in the active power output of NW_HSPP1 to balance the changing demand. This leads to a frequency change at its connecting busbar which is opposite to that of the changing load, Fig. 6a. The HSPPs in the other areas are controlled by their AGCs only to provide partial IR and PCR, as shown in Fig. 6b & c. Hence, they follow the load's frequency and voltage angle change, causing the change in their active power outputs to be much smaller than NW_HSPP1. Minor power oscillations can be observed between HSPPs in the same control area (e.g. SW), which can be resolved with improved damping.

Fig. 7 illustrates the power exchanged by each control area with its neighbors. This can be calculated by summing the power flows through all the interconnections linked with each area. These values are indicated in Fig. 1, with the red arrows indicating the direction of the power flow. Positive values in Fig. 7 indicate power entering a control area and vice versa.

In the absence of the AGC, when load 03 in NW initially increases, power infeed to NW increases as well, Fig. 7a. This is because of the increased output of all the HSPPs in NE, SW and SE, which transfer additional power to NW. Consequently, the power flow to NE reduces while the dispatch from SW and SE increases. Alternatively, when the power consumption decreases, the dispatch from SW and SE reduces. Power flow from NE to NW drops significantly, leading to a lower infeed to NW. Since the magnitude of this reduction is greater than the decrease in power flow from SW to NE and SE to NE, there is a net increase in power entering the control area NE. At a steady state, the net increase in power consumption at NW is satisfied by the increased dispatches from all control areas, leading to a constant deviation in interchange power from the respective initial setpoints in every control area.

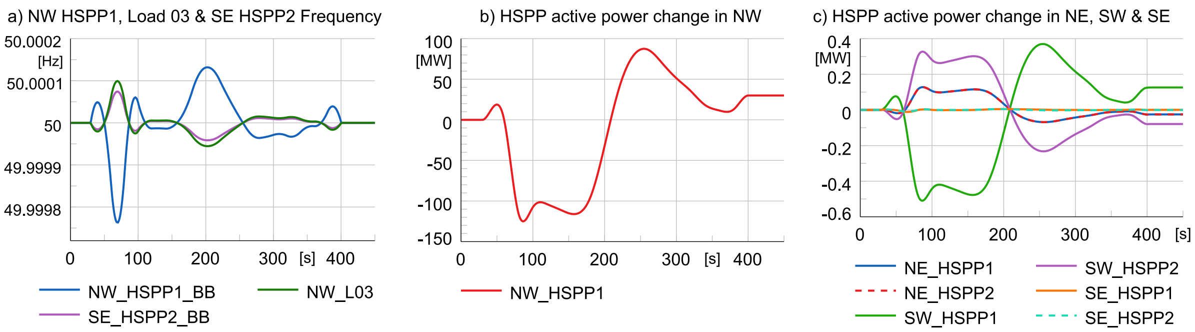

Fig. 6. a) Frequency changes at load 03, NW HSPP 1 and SE HSPP2 busbars, b) & c) Resulting generator responses in different control areas **with AGC**

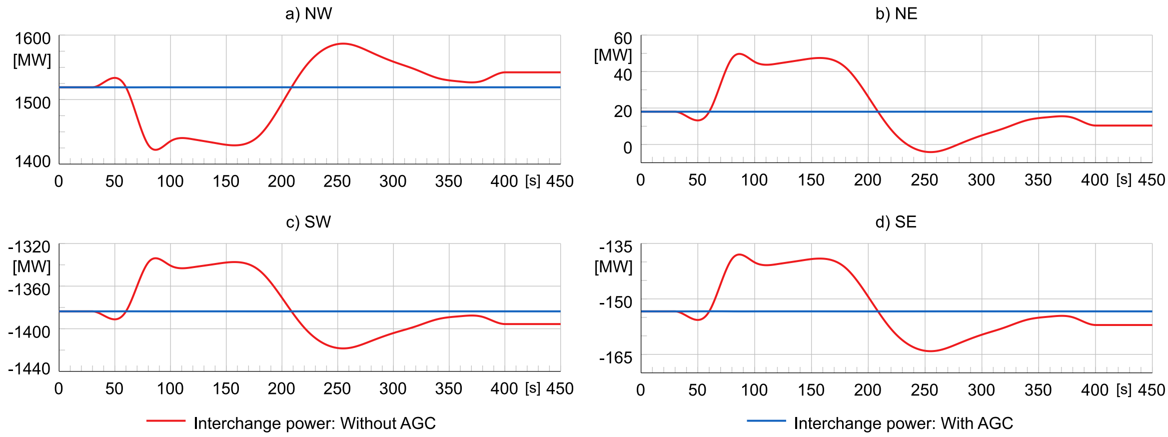

Fig. 7. Exchange power in the respective control areas **with and without AGC**

Once the AGC is activated, the exchange power is always controlled to its initial setpoint. There are slight variations in the interchange power after IR and PCR provision in response to every load change. However, this is difficult to notice in Fig. 7 due to the scale being adapted to compare the interchange power during the two cases.

Conclusion

The HSPP has two different modes of operation, i.e., with and without AGC. When an AGC is not considered, the HSPP keeps its voltage angle constant and provides the required IR and PCR. There is no control over the interchange power between control areas. To include this functionality, the HSPP operates with an AGC and autonomously switches its mode of operation from slack to PQ. This enables the power plant to maintain the exchange power at scheduled values according to previously agreed power contracts. Additional simulations are required with detailed modeling of the HSPP internal storages to test the effect of this control mechanism on the HSPP components. Such analyses will help to determine the size of the HSPP storages and converters, which is a key factor in determining the power plant's market compatibility.

References

[1] Bundesregierung, Energy and Climate Protection. (2023) Renewable energy sources act 2023.

[2] A. S. Chuang and C. Schwaegerl, "Ancillary services for renewable integration," in *2009 CIGRE/IEEE PES Joint Symposium Integration of Wide-Scale Renewable Resources Into the Power Delivery System*, 2009, pp. 1–1.

[3] P. Gerdun, N. Ahmed, V. Vernekar, M. Töpfer, and H. Weber, "Dynamic operation of a storage power plant (spp) with voltage angle control as ancillary service," in *2019 International Conference on Smart Energy Systems and Technologies (SEST)*, 2019, pp. 1–6.

[4] H. Weber, N. Ahmed, and P. Baskar, "Nodal voltage angle control of power systems with renewable sources, storages and power electronic converters," in *2018 International Conference on Smart Energy Systems and Technologies (SEST)*. IEEE, 2018, pp. 1–6.

[5] DIgSILENT GmbH, "400 kv transmission system," in *DIgSILENT PowerFactory 2022*, 2022.

[6] N. Ahmed, P. Gerdun, and H. Weber, "Active power control based on hydrogen availability in a storage power plant," *IFAC-PapersOnLine*, vol. 53, no. 2, pp. 12 708–12 713, 2020.

[7] M. Töpfer, N. Ahmed, and H. Weber, "Dimensioning the internal components of a hydrogen storage power plant," in *2020 International Conference on Smart Energy Systems and Technologies (SEST)*. IEEE, 2020, pp. 1–6.

[8] R. Zhang, J. Fang, and Y. Tang, "Inertia emulation through supercapacitor energy storage systems," in *2019 10th International Conference on Power Electronics and ECCE Asia (ICPE 2019-ECCE Asia)*. IEEE, 2019, pp. 1365–1370.

[9] M. G. Dozein and P. Mancarella, "Frequency response capabilities of utility-scale battery energy storage systems, with application to the august 2018 separation event in australia," in *2019 9th International Conference on Power and Energy Systems (ICPES)*. IEEE, 2019, pp. 1–6.

[10] D. Teichmann, W. Arlt, P. Wasserscheid, and R. Freymann, "A future energy supply based on liquid organic hydrogen carriers (lohc)," *Energy & Environmental Science*, vol. 4, no. 8, pp. 2767–2773, 2011.

[11] P. S. Kundur, *Power system stability and control*. McGraw-Hill Education, 2022.